

A Reconfigurable FACTS System for University Laboratories

L. Dong, *Student Member, IEEE*, M. L. Crow, *Senior Member, IEEE*, Z. Yang, *Member, IEEE*, C. Shen, *Member, IEEE*,
L. Zhang, *Member, IEEE*, and S. Atcitty

Abstract—To fully understand the dynamic performance of the multiple flexible ac transmission systems (FACTS) devices, a hardware setup is needed to complement software simulation for university research laboratories. This paper presents the schematic and basic controls of a reconfigurable FACTS system that can be used to realize the major voltage-sourced-converter FACTS topologies: the StatCom, the static synchronous series compensator (SSSC), and the unified power-flow controller (UPFC). Furthermore, the state models and control algorithms for the FACTS devices are proposed. The digital signal processor (DSP)-based control system enables new control methods to be rapidly implemented. The comparison of the experimental and simulation results is also provided to verify the proposed controls. The paper culminates in a list of suggested experiments appropriate for an elective/graduate course in electric power systems.

Index Terms—Control, flexible ac transmission system, laboratory development.

I. INTRODUCTION

THE RAPID development of the high-power electronics industry has made flexible ac transmission system (FACTS) devices viable and attractive for utility applications. FACTS devices have been shown to be effective in controlling power flow and damping power system oscillations [1]. Several installations of FACTS devices are currently in service in Japan, Brazil, the U.S., and other locations worldwide. Although considerable FACTS research work has concentrated on developing control strategies via simulation, there is a general lack of experimental verification of many of the proposed controls. In order to fully understand how to effectively incorporate FACTS devices into existing power systems, a hardware prototype for verification is necessary in addition to software simulation. Experimental studies provide valuable data to evaluate models, test proposed control algorithms, and analyze dynamic performance. Furthermore, experimental studies provide the basis with which to predict the device performance in the actual power system operation.

This paper provides the schematic for a laboratory scale reconfigurable FACTS system including simple proportional/integral (PI)-based control methods for each topology. These con-

Manuscript received June 9, 2003. This work was supported in part by the National Science Foundation under Grant ECS-9988868 and in part by the Department Of Energy Storage Program through Sandia National Laboratories under Grant BD-0071-D.

L. Dong, M. L. Crow, Z. Yang, C. Shen, and L. Zhang are with the Electrical and Computer Engineering Department, University of Missouri-Rolla, Rolla, MO 65409-0040 USA.

S. Atcitty is with Sandia National Laboratories, Albuquerque, NM 87185 USA.

Digital Object Identifier 10.1109/TPWRS.2003.821022

TABLE I
GLOSSARY OF ACRONYMS

CSGS	- Control Signal Generation Subsystem
DAS	- Data Acquisition System
DSP	- Digital Signal Processing
FACTS	- Flexible AC Transmission System
ISA	- Industry Standard Architecture
PC	- Personal Computer
PI	- Proportional-Integral
PWM	- Pulse Width Modulation
StatCom	- Static Synchronous Compensator
SSSC	- Static Series Synchronous Compensator
SVC	- Static Var Compensator
UPFC	- Unified Power Flow Controller
VSC	- Voltage Source Converter

trols can be easily replaced by more sophisticated controls via the described PC-DSP-based real-time control system. Specifically, the following aspects will be described:

- schematic for the reconfigurable FACTS system;
- description of the real-time control system;
- state models for the StatCom, static synchronous series compensator (SSSC), and unified power-flow controller (UPFC);
- PI controls for the StatCom, SSSC, and UPFC;
- comparison of experimental and simulation results.

Table 1 provides a list of acronyms used throughout.

II. RECONFIGURABLE FACTS SYSTEM

Fig. 1 shows the reconfigurable hardware setup that has been built at the University of Missouri-Rolla. The four primary circuit breakers are used to manually connect and disconnect the StatCom/SSSC/UPFC from the test system. They provide a flexible way to emulate different FACTS topologies. With switches S_2 and S_3 open, and S_1 and S_4 closed, the FACTS device operates in the StatCom topology. With S_2 and S_3 closed, S_1 and S_4 open, the SSSC topology is realized. With all of the switches except S_1 closed, the UPFC topology can be configured. The experimental FACTS devices can also be interfaced with an external energy storage system across the dc capacitor to provide active power support. The FACTS control system consists of two three-phase inverters, LC filters, and two transformers. Two resistor and inductor pairs (R_1, L_1 and R_2, L_2) simulate a midlength transmission line. The phase shift between the two buses is approximately 30° to provide active power flow. The parameter values of the hardware setup are given in Table II. The parameters R_{shunt} and L_{shunt} refer to the shunt transformer. The series parameters refer to the series

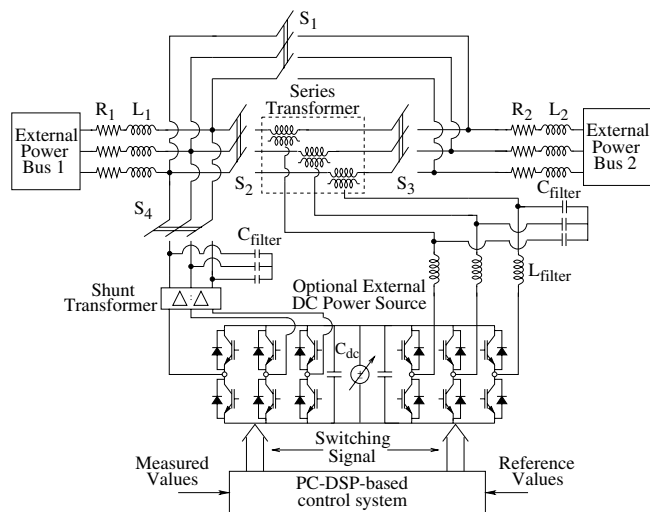


Fig. 1. FACTS laboratory configuration.



Fig. 2. StatCom rack with graphical user interface.

coupling transformer. Additional circuit information is given in the Appendix. The StatCom with graphical user interface is shown in Fig. 2. The transformer is housed in the bottom of the cabinet. The middle portion houses the VSC, including power supplies. The top rack houses the data acquisition and protection system.

The typical control procedure for the FACTS device is: 1) compare the actual voltage, current, and power with the target value; 2) implement the desired control strategy; 3) send the digital control signal to switch the inverter. A PC-DSP-based real-time control system has been developed to efficiently implement the control procedure. This system was chosen for the following features. It provides: 1) an accurate measurement system that can be used to perform fast and reliable signal processing; 2) enough computational power to implement the control algorithm and output the desired control signals; and 3) easy implementation with a PC user interface.

The PC-DSP-based control system includes a host PC, two signal processing boards with an embedded 40-MHz TI TMS32051, and two interface boards. The two DSP boards communicate with the master PC via an industry-standard-architecture (ISA) bus. Fig. 3 shows the master-slave architecture.

TABLE II
SYSTEM PARAMETERS

Test System		FACTS	
Parameter	Value	Parameter	Value
R_1, R_2	0.5Ω	R_{shunt}	0.6267Ω
L_1, L_2	$0.016H$	L_{shunt}	$0.00147H$
L_{filter}	$0.004H$	R_{series}	0.0104Ω
C_{filter}	$100\mu F$	L_{series}	$102\mu H$
		C_{dc}	$940\mu F$

The PC system provides real-time monitoring, control, coordination, and protection for the two DSP-based slave subsystems. The PC also provides online and offline analysis of the FACTS devices. The main task of the data acquisition system (DAS) is to acquire and preprocess eight- or 16-channel analog signals that are measured through voltage and current sensors from the specified FACTS device. Real-time signal processing such as digital filtering, phasor calculation, and system frequency measurement are also implemented in the DAS subsystem. The processed data (active and reactive power, rms voltages, and currents) are exported to the host PC for control algorithm processing. Since these aspects reside in the host PC, different control algorithms can be programmed in C++ and implemented and modified rapidly. The DSP-based pulsewidth-modulation (PWM) control signal generation subsystem (CSGS) is capable of generating up to 12 programmable switching signals to the inverters with adjustable blanking time. The FACTS device fault detection and protection are also accomplished in the CSGS. An LV25-P voltage sensor and a CLN-25 current sensor are used to monitor the three-phase analog line-to-line voltages and line currents. With galvanic isolation between the high-voltage circuit and the secondary output electronic circuit, the sensor circuits provide safe electronic measurements with good accuracy.

PWM was chosen as the primary switching approach for this laboratory system for several reasons. Traditional high-voltage FACTS devices use 24 or 48 switches gate turn-off thyristors (GTOs) coupled through sophisticated transformers to achieve the appropriate phase shifts. Building a comparable FACTS device in the laboratory would prove too costly for most universities due to the cost of the switches and the customized transformers. Second, as power electronics become increasingly faster and cheaper, it is feasible to speculate that industrial FACTS devices will also utilize PWM in the future.

The main hardware components of the DAS are shown in Fig. 4. The 8/16 scaled analog data input channels from the external high power circuit are first isolated by ISO124 chips and then converted to digital signals. The StatCom and SSSC each require eight input channels whereas the UPFC utilizes all 16 input channels. All of the analog data inputs are imported and stored in the host PC. The PC onboard timer is used to manage the data-acquisition sampling time. The corresponding interrupt channels are shown as INT#. The experimental DAS is shown in Fig. 5. Note that both digital (top) and analog (bottom) signals are processed with the same board.

The DSP-based PWM CSGS is capable of generating up to 12 programmable switching signals to gate the inverters with adjustable blanking time. The fault detection and protection pro-

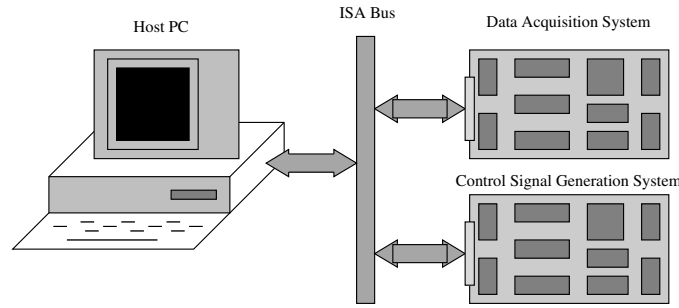


Fig. 3. DSP system architecture.

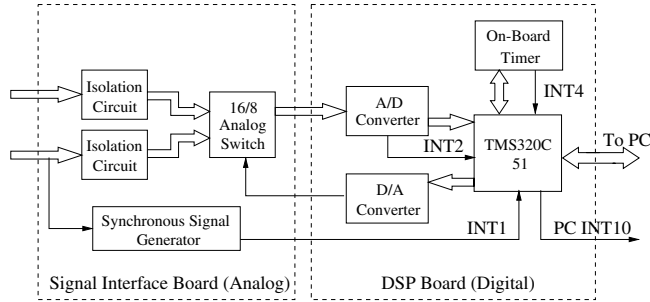


Fig. 4. Data-acquisition circuit.

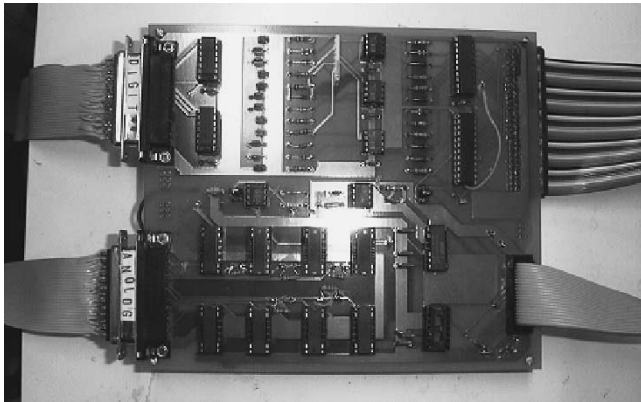


Fig. 5. Data-acquisition subsystem.

cesses are also built into the CSGS. Fig. 6 shows the CSGS hardware configuration. The control signals generated by the CSGS are output to an extended I/O device. With the built-in latch feature, the valid logic signals can be picked from the buffered I/O data bus. The adjustable blanking time feature is utilized to avoid shoot-through and cross conduction current in the inverter legs. Generally, the logic-level control signals are not powerful enough to directly switch the insulated gate bipolar transistors (IGBTs); therefore, a Fuji EXB840 IGBT driver chip is used as an interface.

III. FACTS MODELING AND CONTROL

One of the main objectives of developing a laboratory prototype FACTS device is to provide the ability to experimentally verify proposed controls. Most controls are first developed and simulated using a set of dynamics that describe each FACTS device. The dynamic models of the FACTS devices are nonlinear and nonconstant due to the nature of the inverter

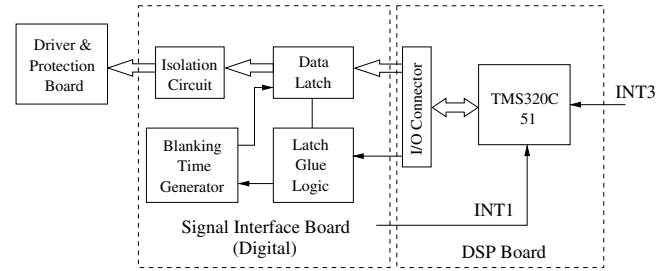


Fig. 6. Control signal generation subsystem.

switching. In addition, the dynamics of the inverter switches are much faster than the dynamics of interest in the power system. Therefore, it is desirable to use a set of simplified state-based models for the FACTS devices that are sufficiently accurate in that they provide accurate representation of the true hardware system, yet simple enough for implementation in a power system simulation. This section will provide experimentally verified simple models for the static synchronous compensator (StatCom), SSSC, and UPFC. Although at a reduced voltage level, a laboratory FACTS device can provide significant insight into the actual behavior of FACTS devices in a multimachine power system. By connecting the FACTS devices to synchronous machines or induction machines, the dynamic interaction between the devices can be analyzed and new controls rapidly synthesized and implemented via the DSP-based control system. The experimental verification of the state-space models presented in this section lends credence to using these simplified models for large-scale system analysis. Second, while the developed laboratory system has a limited voltage and power rating, the basic control of the dynamic behavior does not change when scaled to larger systems.

A. StatCom

The StatCom is a voltage-sourced-converter (VSC)-based shunt-connected device. By injecting a current of variable magnitude in quadrature with the line voltage, the StatCom can inject reactive power into the power system. The StatCom does not employ capacitor or reactor banks to produce reactive power as does the SVC, but instead uses a capacitor to maintain a constant dc voltage for the inverter operation. An equivalent circuit for the StatCom is shown in Fig. 7. The loop equations for the circuit may be written in vector form as

$$\frac{d}{dt} i_{abc} = -\frac{R_s}{L_s} i_{abc} + \frac{1}{L_s} (E_{abc} - V_{abc}) \quad (1)$$

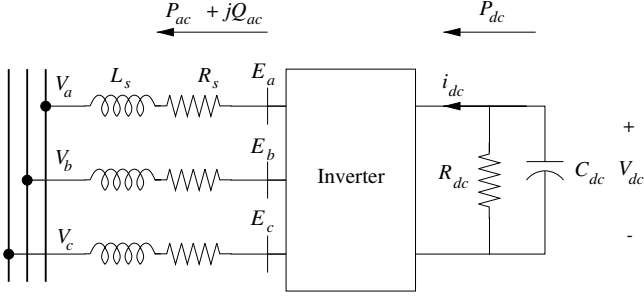


Fig. 7. Equivalent circuit of the StatCom.

where R_s and L_s represent the StatCom transformer losses (given as R_{shunt} and L_{shunt} in Table II), E_{abc} are the inverter ac side phase voltages, V_{abc} are the system-side phase voltages, and i_{abc} are the phase currents. The output of the StatCom is given by

$$E_a = kV_{dc} \cos(\omega t + \alpha) \quad (2)$$

where V_{dc} is the voltage across the dc capacitor, k is the modulation gain, and α is the injected voltage phase angle. By defining a proper synchronous reference frame, the dynamic model can be simplified. The reference frame coordinate is defined in which the d -axis is always coincident with the instantaneous system voltage vector and the q -axis is in quadrature with it. By transforming the system model to this reference frame, the StatCom equations at bus i can be written as [2], [3]

$$\begin{aligned} \frac{1}{\omega_s} \frac{d}{dt} i_d &= -\frac{R_s}{L_s} i_d + \frac{\omega}{\omega_s} i_q \\ &+ \frac{k}{L_s} \cos(\alpha + \theta_i) V_{dc} - \frac{V_i}{L_s} \cos \theta_i \end{aligned} \quad (3)$$

$$\begin{aligned} \frac{1}{\omega_s} \frac{d}{dt} i_q &= -\frac{R_s}{L_s} i_q - \frac{\omega}{\omega_s} i_d \\ &+ \frac{k}{L_s} \sin(\alpha + \theta_i) V_{dc} - \frac{V_i}{L_s} \sin \theta_i \end{aligned} \quad (4)$$

$$\begin{aligned} \frac{C_{dc}}{\omega_s} \frac{d}{dt} V_{dc} &= -k \cos(\alpha + \theta_i) i_d \\ &- k \sin(\alpha + \theta_i) i_q - \frac{V_{dc}}{R_{dc}} \end{aligned} \quad (5)$$

where i_d and i_q are the injected dq StatCom currents, V_{dc} is the voltage across the dc capacitor, R_{dc} represents the switching losses, R_s and L_s are the coupling transformer resistance and inductance, respectively, and the StatCom rms bus voltage is $V_i \angle \theta_i$. The power balance equations at the StatCom bus are

$$\begin{aligned} 0 &= V_i (i_d \cos \theta_i + i_q \sin \theta_i) \\ &- V_i \sum_{j=1}^n V_j Y_{ij} \cos(\theta_i - \theta_j - \phi_{ij}) \end{aligned} \quad (6)$$

$$\begin{aligned} 0 &= V_i (i_d \sin \theta_i - i_q \cos \theta_i) \\ &- V_i \sum_{j=1}^n V_j Y_{ij} \sin(\theta_i - \theta_j - \phi_{ij}) \end{aligned} \quad (7)$$

where the summation terms represent the power flow equations, $Y_{ij} \angle \phi_{ij}$ is the (i, j) th element of the admittance matrix, and

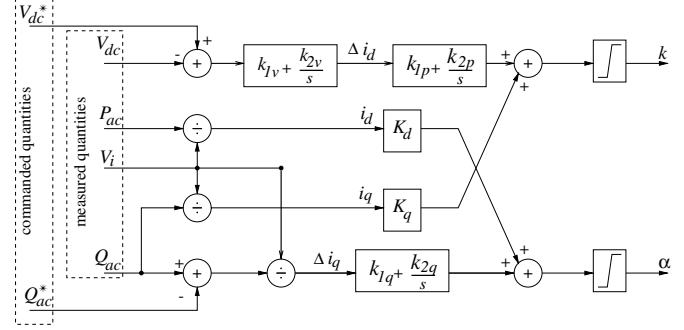


Fig. 8. StatCom control.

n is the number of buses in the system. The first set of terms indicates the active and reactive powers injected by the StatCom, respectively, whereas the summation of power terms on the right are the power-flow equations of the power system.

The control objectives for the StatCom are to provide independent reactive power support and to maintain constant dc capacitor voltage. This is best accomplished by regulating the PWM switching commands to alter the modulation index and phase angle in (2). One easily implemented control is shown in Fig. 8. In this control, the input signals V_{dc} and Q are compared against reference values and used to compute the error signals in i_d and i_q . A PI-based control is then used to produce the control signals k and α [4]. In reality, both the firing angle α and modulation gain k are impacted by changes in i_d and i_q . However, since α is more strongly correlated to changes in i_q and k is more strongly correlated to changes in i_d , the cross coupling terms can be neglected ($K_d = K_q = 0$) leading to a decoupled control approach.

IV. SSSC

The SSSC is a VSC-based serial FACTS device that can provide capacitive or inductive compensation independent of the line current [5], [6]. The SSSC typically has the same power electronics topology as the StatCom. However, it is incorporated into the ac power system through a series coupling transformer as opposed to the shunt transformer found in the StatCom. The series transformer is used to inject an independently controlled voltage in quadrature with the line current for the purpose of increasing or decreasing the overall reactive voltage drop across the line and, thereby, controlling the transmitted power. In essence, the SSSC may be considered to be a controllable effective line impedance [5]. Since the SSSC has a VSC topology, the dc capacitor is used to maintain the dc voltage, giving the SSSC the ability to increase or decrease the transmitted power across the line by a fixed fraction of the maximum power, independent of the phase angle. As a result of the SSSC's ability for reactive power generation or absorption, it makes the surrounding power system impervious to classical subsynchronous resonances.

Fig. 9 shows an SSSC located at the midpoint of a transmission line. The transmission line is modeled with lumped impedances. The voltages $V_1 \angle \theta_1$ and $V_2 \angle \theta_2$ are the midpoint voltages on each side of the SSSC, and $V_{inj} \angle \theta_{inj}$ represents the voltage

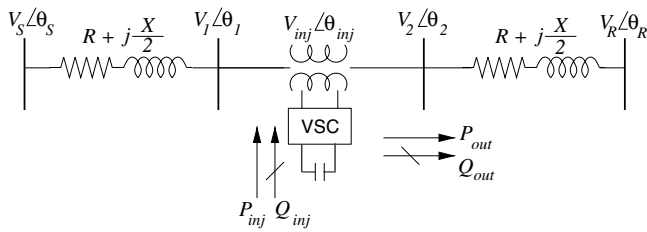


Fig. 9. Two-bus system with midpoint SSSC.

injected by the controller. The SSSC model is similar to that of the StatCom

$$\frac{1}{\omega_s} \frac{d}{dt} i_d = -\frac{R_s}{L_s} i_d + \frac{\omega}{\omega_s} i_q + \frac{k}{L_s} \cos(\alpha + \theta_1) V_{dc} - \frac{1}{L_s} (V_2 \cos \theta_2 - V_1 \cos \theta_1) \quad (8)$$

$$\frac{1}{\omega_s} \frac{d}{dt} i_q = -\frac{R_s}{L_s} i_q - \frac{\omega}{\omega_s} i_d + \frac{k}{L_s} \sin(\alpha + \theta_1) V_{dc} - \frac{1}{L_s} (V_2 \sin \theta_2 - V_1 \sin \theta_1) \quad (9)$$

$$\frac{C}{\omega_s} \frac{d}{dt} V_{dc} = -k \cos(\alpha + \theta_1) i_d - k \sin(\alpha + \theta_1) i_q - \frac{V_{dc}}{R_{dc}} \quad (10)$$

where $V_1 \angle \theta_1$ and $V_2 \angle \theta_2$ are the terminal voltages of the SSSC. The power balance equations at the sending end of the SSSC (bus 1) are given by

$$0 = -V_1 (i_d \cos \theta_1 + i_q \sin \theta_1) - V_1 \sum_{j=1}^n V_j Y_{1j} \cos(\theta_1 - \theta_j - \phi_{1j}) \quad (11)$$

$$0 = -V_1 (i_d \sin \theta_1 - i_q \cos \theta_1) - V_1 \sum_{j=1}^n V_j Y_{1j} \sin(\theta_1 - \theta_j - \phi_{1j}) \quad (12)$$

and at the receiving end (bus 2)

$$0 = V_2 (i_d \cos \theta_2 + i_q \sin \theta_2) - V_2 \sum_{j=1}^n V_j Y_{2j} \cos(\theta_2 - \theta_j - \phi_{2j}) \quad (13)$$

$$0 = V_2 (i_d \sin \theta_2 - i_q \cos \theta_2) - V_2 \sum_{j=1}^n V_j Y_{2j} \sin(\theta_2 - \theta_j - \phi_{2j}). \quad (14)$$

When PWM switching is used to govern the switching, then

$$V_{inj} = k V_{dc} = k_{tr} m_a V_{dc} \quad (15)$$

$$\theta_{inj} = \theta_1 + \alpha \quad (16)$$

where k and α are the PWM modulation gain and phase shift. The modulation gain k is proportional to the modulation index m_a and k_{tr} which are determined by the modulation method and the serial transformer winding ratio. The range of m_a and α are constrained by the steady-state reactive power capabilities of the controller. Fig. 10 gives the related phasor diagram of the SSSC

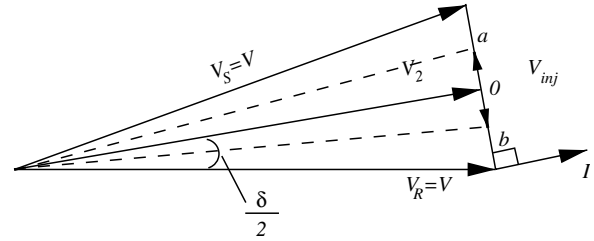


Fig. 10. SSSC phasor diagram.

where it has been assumed that $V_S = V_R = V$ and $\delta = \theta_S - \theta_R$. The phase shift α is referenced to θ_1 since it is not practical to synchronize the injected voltage to the system reference. This diagram can be used as a basis from which to derive a control approach. If losses are neglected, then the injected powers P_{inj} and Q_{inj} , and the output powers P_{out} and Q_{out} can be related as follows:

$$P_{inj} = \frac{V_{inj} V}{X} (\sin \theta_{inj} - \sin(\theta_{inj} - \delta)) = \frac{V(E_q - E_q \cos \delta + E_d \sin \delta)}{X} \quad (17)$$

$$Q_{inj} = \frac{V_{inj}}{X} (V \cos(\theta_{inj} - \delta) + V_{inj} - V \cos \theta_{inj}) = \frac{V E_q \cos \delta + V E_q \sin \delta - V E_d + V_{inj}^2}{X} \quad (18)$$

$$P_{out} = \frac{V^2 \sin \delta + V V_{inj} \sin \theta_{inj}}{X} = \frac{V^2 \sin \delta + V E_q}{X} \quad (19)$$

$$Q_{out} = \frac{2 V_{inj} V \cos(\delta - \theta_{inj}) + V_{inj}^2}{2X} = \frac{2V E_d \cos \delta + 2V E_q \sin \delta + V_{inj}^2}{2X} \quad (20)$$

where

$$E_q = V_{inj} \sin \theta_{inj} \quad E_d = V_{inj} \cos \theta_{inj} \quad V_{inj}^2 = E_d^2 + E_q^2.$$

Since $P_{inj} = 0$, (17) indicates that

$$\theta_{inj} = \pm \frac{\pi}{2} + \frac{\delta}{2}.$$

Note that the compensated SSSC voltage vector V_2 will remain on the line ab since the injected voltage V_{inj} must be perpendicular to the current I at all times. The phasor diagram and the relationships described above provide a framework in which to develop a systematic control scheme for the SSSC.

The power-flow control capability of an SSSC is constrained by its pure reactive power compensation capability during steady-state operation. The traditional approach to PWM-based SSSC control is to use the modulation index m_a to adjust the compensated apparent impedance, while using the phase shift to charge or discharge the dc capacitor [7]. Since the control effect of m_a and α interact with each other, it is desirable to introduce two new constrained decoupled control variables ΔE_d and ΔE_q to obtain the control target, where

$$\Delta P_{inj} = \frac{V}{X} (\Delta E_q (1 - \cos \delta) + \Delta E_d \sin \delta).$$

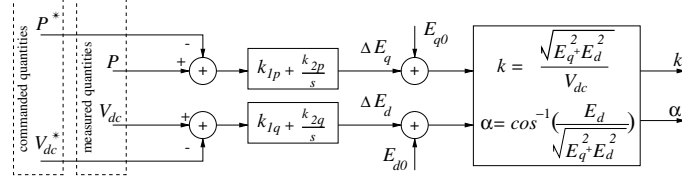


Fig. 11. SSSC control.

Under normal operations, the phase angle between adjacent buses is relatively small. Therefore, since δ is small, then $(1 - \cos \delta) \approx 0$ and

$$\Delta P_{inj} \approx \frac{V}{X} \Delta E_d \sin \delta. \quad (21)$$

Limited by the lack of an active power source on the dc side from which to absorb or inject energy, it is therefore important to control the injected active power close to zero to maintain near constant dc voltage across the VSC capacitor. A nearly constant dc voltage is important since it directly affects the control speed and effectiveness of the SSSC. From (21), ΔE_d is the main factor in affecting the injected active power, thus ΔE_d can be used to adjust the dc capacitor voltage around its reference value. By combining the controls for dc voltage and transmission line active power flow, a constrained decoupled PI control algorithm for the SSSC is given by

$$\Delta E_q = k'_{pp} \Delta P_2 + k'_{pi} \int \Delta P_2 dt \quad (22)$$

$$\Delta E_d = k_{vp} \Delta V_{dc} + k_{vi} \int \Delta V_{dc} dt. \quad (23)$$

In implementation, these quantities are combined with the initial operating point and converted into a modulation index m_a and phase shift α such that

$$m_a = \frac{\sqrt{E_d^2 + E_q^2}}{k_{tr} V_{dc}}$$

$$\alpha = \begin{cases} \sin^{-1} \left(\frac{E_q}{\sqrt{E_d^2 + E_q^2}} \right) - \theta_1, & E_d > 0 \\ \pi - \sin^{-1} \left(\frac{E_q}{\sqrt{E_d^2 + E_q^2}} \right) - \theta_1, & E_d < 0; E_q > 0 \\ -\pi - \sin^{-1} \left(\frac{E_q}{\sqrt{E_d^2 + E_q^2}} \right) - \theta_1, & E_d < 0; E_q < 0 \end{cases}$$

where $E_q = E_{q0} + \Delta E_q$, $E_d = E_{d0} + \Delta E_d$, $E_{q0} = k_{tr} m_{a0} V_{dc} \sin(\alpha + \theta_1)$, and $E_{d0} = k_{tr} m_{a0} V_{dc} \cos(\alpha + \theta_1)$. This control is summarized in Fig. 11.

V. UPFC

The UPFC is the most versatile FACTS device. It consists of a combination of a shunt and series branches (StatCom and SSSC) connected through the dc capacitor. The series-connected inverter injects a voltage with controllable magnitude and phase angle in series with the transmission line, therefore providing real and reactive power to the transmission line. The shunt-connected inverter provides the real power drawn by the series branch and the losses and can independently provide reactive

compensation to the system. The UPFC model is a combination of the StatCom and SSSC models

$$\frac{1}{\omega_s} \frac{d}{dt} i_{d1} = \frac{k_1 V_{dc}}{L_{s1}} \cos(\alpha_1 + \theta_1) + \frac{\omega}{\omega_s} i_{q1} - \frac{R_{s1}}{L_{s1}} i_{d1} - \frac{V_1}{L_{s1}} \cos \theta_1 \quad (24)$$

$$\frac{1}{\omega_s} \frac{d}{dt} i_{q1} = \frac{k_1 V_{dc}}{L_{s1}} \sin(\alpha_1 + \theta_1) - \frac{R_{s1}}{L_{s1}} i_{q1} - \frac{\omega}{\omega_s} i_{d1} - \frac{V_1}{L_{s1}} \sin \theta_1 \quad (25)$$

$$\frac{1}{\omega_s} \frac{d}{dt} i_{d2} = -\frac{R_{s2}}{L_{s2}} i_{d2} + \frac{\omega}{\omega_s} i_{q2} + \frac{k_2}{L_{s2}} \cos(\alpha_2 + \theta_1) V_{dc} - \frac{1}{L_{s2}} (V_2 \cos \theta_2 - V_1 \cos \theta_1) \quad (26)$$

$$\frac{1}{\omega_s} \frac{d}{dt} i_{q2} = -\frac{R_{s2}}{L_{s2}} i_{q2} - \frac{\omega}{\omega_s} i_{d2} + \frac{k_2}{L_{s2}} \sin(\alpha_2 + \theta_1) V_{dc} - \frac{1}{L_{s2}} (V_2 \sin \theta_2 - V_1 \sin \theta_1) \quad (27)$$

$$\frac{C}{\omega_s} \frac{d}{dt} V_{dc} = -k_1 \cos(\alpha_1 + \theta_1) i_{d1} - k_1 \sin(\alpha_1 + \theta_1) i_{q1} - k_2 \cos(\alpha_2 + \theta_1) i_{d2} - k_2 \sin(\alpha_2 + \theta_1) i_{q2} - \frac{V_{dc}}{R_{dc}}. \quad (28)$$

The power balance equations at bus 1 are given by

$$0 = V_1 ((i_{d1} - i_{d2}) \cos \theta_1 + (i_{q1} - i_{q2}) \sin \theta_1) - V_1 \sum_{j=1}^n V_j Y_{1j} \cos(\theta_1 - \theta_j - \phi_{1j}) \quad (29)$$

$$0 = V_1 ((i_{d1} - i_{d2}) \sin \theta_1 - (i_{q1} - i_{q2}) \cos \theta_1) - V_1 \sum_{j=1}^n V_j Y_{1j} \sin(\theta_1 - \theta_j - \phi_{1j}) \quad (30)$$

and at bus 2

$$0 = V_2 (i_{d2} \cos \theta_2 + i_{q2} \sin \theta_2) - V_2 \sum_{j=1}^n V_j Y_{2j} \cos(\theta_2 - \theta_j - \phi_{2j}) \quad (31)$$

$$0 = V_2 (i_{d2} \sin \theta_2 - i_{q2} \cos \theta_2) - V_2 \sum_{j=1}^n V_j Y_{2j} \sin(\theta_2 - \theta_j - \phi_{2j}). \quad (32)$$

The UPFC has three control parameters: the magnitude and angle of the injected voltage and the shunt reactive current. Active and reactive power flow control can be controlled independently by injecting a series voltage with an appropriate magni-

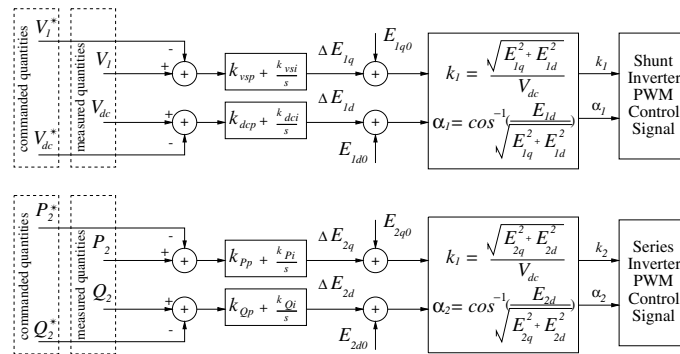


Fig. 12. UPFC control.

tude and angle. In the synchronous rotating dq reference frame, the injected voltage can be split into E_d and E_q . By controlling E_d and E_q properly, different active and reactive power flows can be achieved. Essentially, the control of the UPFC is a combination of the StatCom and SSSC as shown in Fig. 12.

VI. FACTS EXPERIMENTS

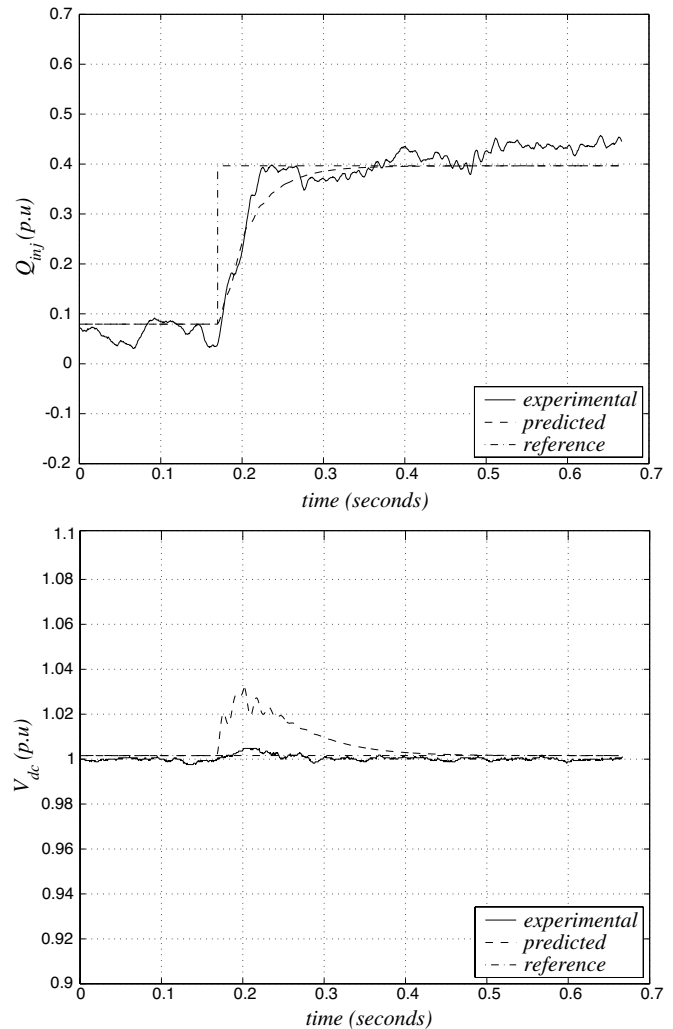
In this section, several illustrative experiments will be described to show how students can use the FACTS laboratory to study the behavior of FACTS devices on a system and the impact of the controls.

A. StatCom Experiments

A first experiment with the StatCom is to verify that the StatCom will respond appropriately to a step change in bus voltage reference (V^*). In a second experiment, students are asked to modify the control to track a step change in reactive power. The results of this experiment are shown in Fig. 13. Note the similarity between the experimental and predicted responses and that the experimental system actually responds better than predicted in maintaining constant V_{dc} . This experiment not only validates the control method, but also validates the use of the described StatCom model to predict the dynamic behavior of the system. The influence of the PI control can be observed by the signal overshoot and exponential decay to the reference. This is typical of a PI control response.

B. SSSC Experiments

Similar experiments can be performed with the SSSC. For example, one typical experiment will use the SSSC to change the active power flow across the transmission line. This is one extremely powerful use of the SSSC. This experiment can be used to facilitate a discussion about the use of FACTS devices to impact transmission congestion. The results of the SSSC experiment are shown in Fig. 14. In this experiment, the SSSC is used to increase the active power flow on the transmission line by 25%. Note similar PI control responses to the StatCom. In addition to the effectiveness of the SSSC on active power flow, the students can interpret the corresponding changes in bus voltage (Why does it decrease?) and injected reactive power (Why is the change in Q_{inj} greater than P_{inj} ? Why is reactive power injection used to control the active line power?) and V_{dc} (Why is it important to hold V_{dc} constant?).

Fig. 13. StatCom response to a commanded step change in commanded voltage— Q_{inj} (top), V_{dc} (bottom).

Another use of the SSSC is to damp system transients. Various experiments can be designed to illustrate this benefit. One possible experiment is to use the SSSC with the optional energy storage system to damp the transients induced by an induction motor start up. In this experiment, a three-phase induction motor is suddenly connected to the SSSC receiving end (bus 2). The induction motor is driven by a dc dynamometer. The dynamic response of the SSSC to the sudden change in motor load is shown in Fig. 15. The SSSC control takes effect the instant the

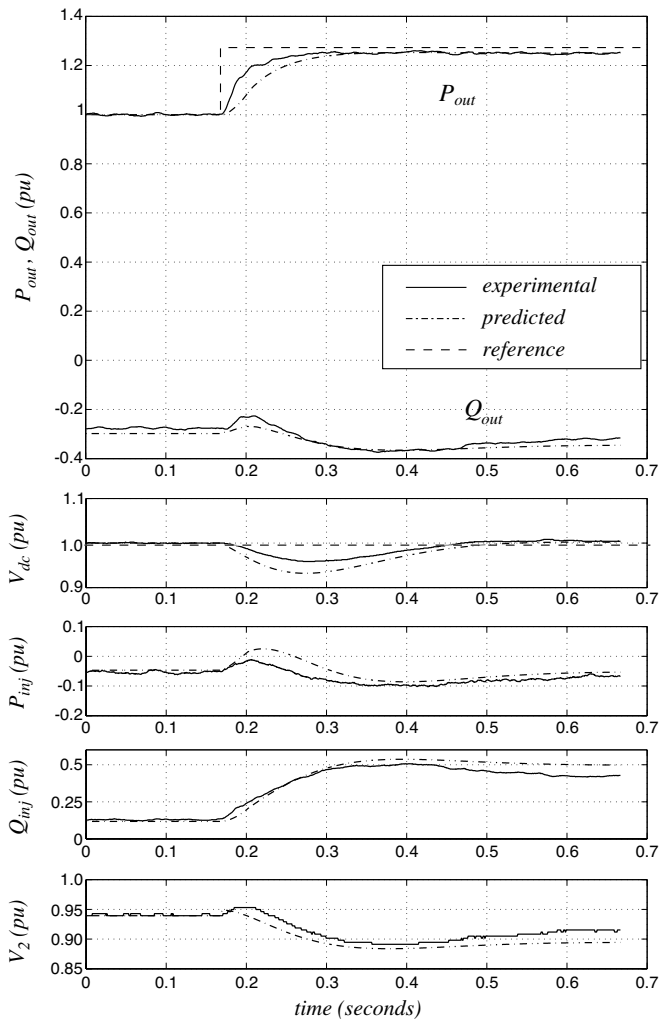


Fig. 14. SSSC response to a commanded step change in transmission line power transfer (P_{out} , Q_{out} , P_{inj} , Q_{inj} , and V_2 top to bottom, respectively).

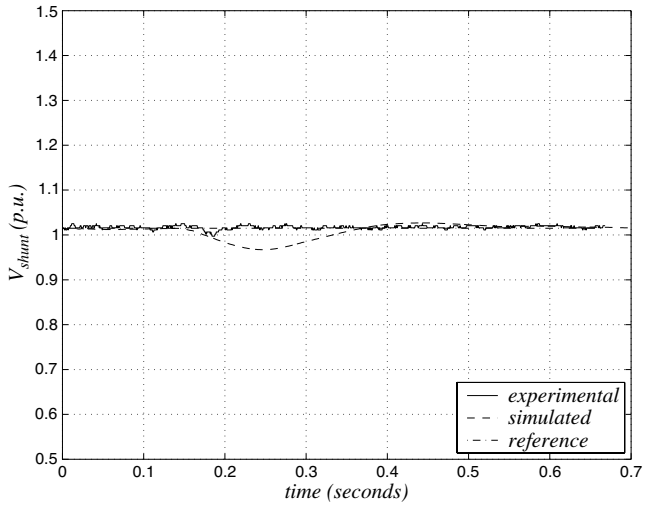
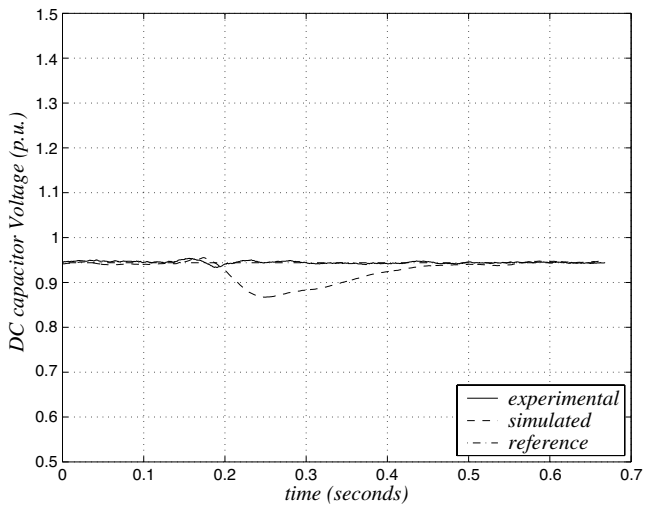
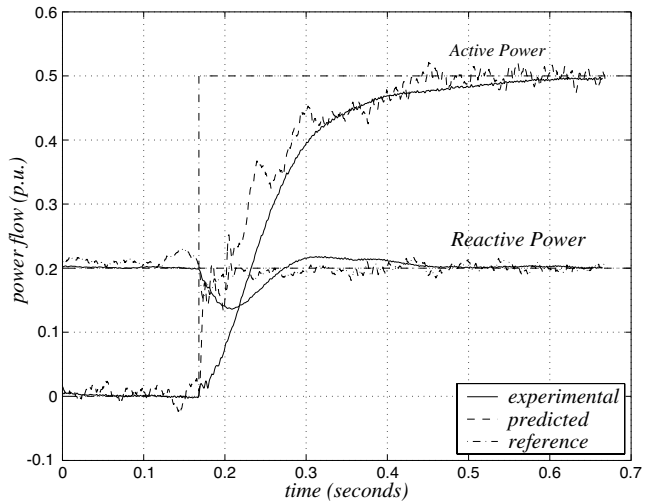


Fig. 16. UPFC response— P_2 , Q_2 (top), V_{dc} (middle), V_1 (bottom).

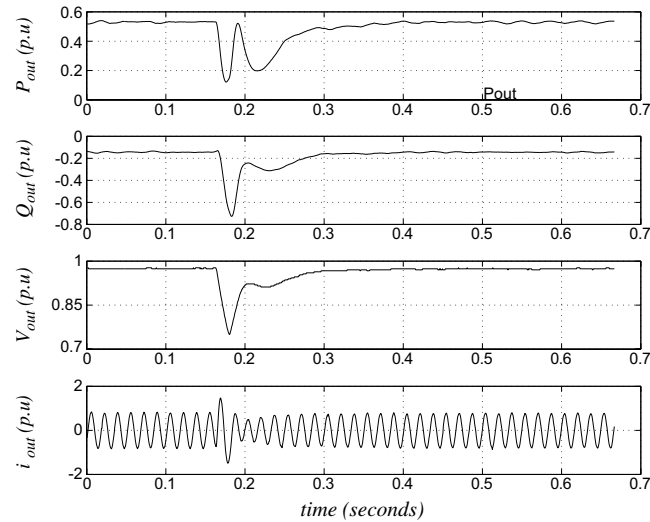


Fig. 15. SSSC response to induction motor switching.

motor load is connected to the system. The SSSC control is designed to hold the transmission line power flow constant. The dynamometer senses and reacts to the speed change in the induction motor by adjusting its output. This is the cause of the second dip in the dynamic response. The SSSC, however, reacts

to this dynamic change as well and brings the transmission line power flow back to the reference value. Only experimental results are shown in Fig. 15 since it is difficult to accurately model and simulate the response of the dynamometer.

C. UPFC Experiments

Experiments with the UPFC combine both aspects of StatCom and SSSC control. A typical first experiment with

TABLE III
CONTROL PARAMETERS

StatCom	V_{dc}	V_{shunt}
	$K_p = 0.1$	$K_p = 0.15$
	$K_i = 0.05$	$K_i = 0.05$
SSSC	P_{line}	Q_{line}
	$K_p = 0.015$	$K_p = 0.015$
	$K_i = 0.05$	$K_i = 0.5$
UPFC Shunt	V_{dc}	V_{shunt}
	$K_p = 0.1$	$K_p = 0.15$
	$K_i = 0.05$	$K_i = 0.05$
UPFC Series	P_{line}	Q_{line}
	$K_p = 0.015$	$K_p = 0.015$
	$K_i = 0.5$	$K_i = 0.5$

the UPFC integrates the previous experiments to change line power and maintain voltages. A set of such results is shown in Fig. 16 where the line power reference is changed. These results are similar to those of the StatCom and SSSC. As with the StatCom, the experimental results are better than the predicted results. This is due in part to the difficulty in accurately extracting the necessary parameters such as R_{dc} which models switching losses.

One advantage of the PC-DSP system is that new controls can be rapidly implemented. Additional experiments can include developing and implementing new controls. Examples of student projects have included the implementation of optimal control for a StatCom and fuzzy logic control for the UPFC.

VII. CONCLUSION

This paper presents a schematic of a reconfigurable VSC-based FACTS laboratory including the DSP-based DAS and signal generator. In addition, this paper includes the set of state space models for each of the FACTS devices. Each device is described by the corresponding differential equations and the power balance equations for the terminal buses. A PI-based controller is developed for each device and then verified experimentally using the reconfigurable laboratory system. Suggestions for student experiments and projects using the controls and laboratory hardware complete the discussion. This laboratory system provides an excellent opportunity to design novel controls rapidly using the provided models and then experimentally verifying their effectiveness.

APPENDIX

TEST CIRCUIT AND CONTROL PARAMETERS

The inverter is rated to 60 kVA. The PWM switching frequency is 1620 Hz. The voltage rating of the test system is 230 V (line–line) at 60 Hz. The Δ – Δ transformer is rated 10 kVA. The series coupling transformer is comprised of three single-phase 2.5:1 5-kVA transformers connected Δ – Y . Table III lists the control parameters of the experimental FACTS devices.

REFERENCES

- [1] R. Koessler, B. Fardanesh, M. Henderson, and R. Adapa, Feasibility studies for StatCon application in New York state, in *FACTS Applications*, pp. 8.52–8.58, 1996.
- [2] C. Schauder and H. Mehta, "Vector analysis and control of advanced static VAR compensators," *Proc. Inst. Elect. Eng., Gen. Transm. Dist.*, vol. 140, no. 4, pp. 299–306, July 1993.
- [3] P. Lehn, "Exact modeling of the voltage source converter," *IEEE Trans. Power Delivery*, vol. 17, pp. 217–222, Jan. 2002.
- [4] Z. Yang, C. Shen, L. Zhang, M. L. Crow, and S. Atcitty, "Integration of a StatCom and battery energy storage," *IEEE Trans. Power Syst.*, vol. 16, pp. 254–260, May 2001.
- [5] L. Gyugyi *et al.*, "Static synchronous series compensator: A solid state approach to the series compensation of transmission lines," *IEEE Trans Power Syst.*, vol. 12, pp. 406–417, Jan. 1997.
- [6] E. V. Larsen *et al.*, "Characteristics and rating considerations of thyristor controlled series compensation," *IEEE Trans Power Delivery*, vol. 9, pp. 992–1000, Apr. 1994.
- [7] B. Rigby, "An improved control scheme for a series-capacitive reactance compensator based on a voltage-source inverter," *IEEE Trans. Ind. Appl.*, vol. 34, pp. 355–363, Mar./Apr. 1998.

L. Dong (S'00) received the B.S. degree in electrical engineering from Hefei University of Technology, Anhui, R.O.C., in 1997, and the M.S. degree from Tianjin University, Tianjin, R.O.C., in 2000. She is currently pursuing the Ph.D. degree in electrical and computer engineering at the University of Missouri-Rolla, Rolla.

Her research interests include FACTS control, placement, and interaction.

M. L. Crow (SM'94) received the B.S.E. degree from the University of Michigan at Ann Arbor, and the Ph.D. degree from the University of Illinois, at Urbana-Champaign.

Currently, she is the Associate Dean for Research and Graduate Affairs and a Professor of Electrical and Computer Engineering at the University of Missouri-Rolla, Rolla. Her research interests include developing computational methods for dynamic security assessment and the application of power electronics in bulk power systems.

Dr. Crow is the Vice-President for Education/Industry relations of the IEEE Power Engineering Society.

Z. Yang (M'00) received the B.S. degrees and the M.S.E.E. degree from Tsinghua University, Beijing, China, in 1994 and 1997, respectively, and the Ph.D. degree in electrical engineering from the University of Missouri-Rolla, Rolla, in 2000.

Currently, he is with Cisco Systems, San Jose, CA. His research interests include power electronics and applications in power systems.

C. Shen (M'00) received the B.S., M.S., and Ph.D. degrees in electrical engineering from Tsinghua University, Beijing, China, in 1993, 1995, and 1998, respectively.

Currently, he is with the faculty at Tsinghua University, Beijing, China. He was with the New England independent system operator (ISO), Holyoke, MA, from 2001 to 2002. His research interests include FACTS control and power system stability.

L. Zhang (M'01) received the B.Sc. degree from Zhejiang University, Zhejiang, China, in June 1994, and the M.S. degree from the North China Electric Power University, China, in 1998, and the Ph.D. degree in electrical engineering from the University of Missouri-Rolla, Rolla, in 2001.

Currently, she is with Cirrus Systems, Austin, TX. Her research areas include FACTS control and power system stability.

S. Atcitty received the B.S. and M.S. degrees in electrical engineering from New Mexico State University, Las Cruces.

Currently, he is a Power Electronics Consultant with Energy Storage System Program at Sandia National Laboratories, Albuquerque, NM. His research interests include high-power electronics and applications in power systems.